Microstructure and Growth Model of Periodic Spindle-Unit BN Nanotubes by Nitriding Fe-B Nanoparticles with Nitrogen/Ammonia Mixture

K. F. Huo, Z. Hu,* J. J. Fu, H. Xu, X. Z. Wang, and Y. Chen

Key Lab for Mesoscopic Materials Science and Jiangsu Provincial Lab of Nanotechnology, Department of Chemistry, Nanjing University, Nanjing 210093, China

Y. N. Lü

College of Materials Science and Engineering, Nanjing University of Technology, Nanjing 210009, China

Received: May 19, 2003; In Final Form: August 7, 2003

Periodic spindle-unit boron nitride (BN) nanotubes with buglelike open-end tips have been found in the product by nitriding Fe-B nanoparticles at 1100 °C with a mixture of nitrogen and ammonia gas. The microstructure was well-characterized by high-resolution transmission electron microscopy (HRTEM) and energy-dispersive X-ray spectroscopy (EDX). The diameter of this BN nanotube shows a decreasing tendency along the growth direction. For each spindle unit, the outer diameter decreases steeply and then increases gradually, accompanied by thinning of the wall thickness along the growth direction. Some spindle units are partially occupied by the iron-containing catalyst particles at the hemispherical-like ends. An improved stress-induced sequential growth model has been reasonably deduced accordingly, with which the formation process of this novel BN nanostructure could be well understood.

Introduction

Inspired by the extreme importance of fullerenes[1] and carbon nanotubes,[2] periodic carbon nanostructures such as strings of graphitic beads,[3] carbon nanochains,[4] and bamboolike carbon nanotubes (CNTs)[5−11] have generated much scientific curiosity, because of their morphological peculiarity and many interesting properties for potential applications in the fields, e.g., electron emission, hydrogen storage, and composites.[12−14] To date, numerous arguments have been postulated to explain the growth of these periodic carbon nanostructures: annealing-induced metal particle migration out of carbon cages;[3] metal-atom evaporation through defects of the outer graphitic carbon;[4] stress induced by the newly formed carbon layers;[5−7] increased surface tension at the nanotube/catalyst interface, because of the decreased carbon concentration in the catalyst particle;[8] periodic instability of the liquid state of the catalyst particle;[9] difference between the nanotube growth rate and the forward velocity of the catalyst particle;[10] and sequential catalytic growth.[11] According to the similarities between graphite and hexagonal BN,[15] the existence of boron nitride nanotubes (BN-NTs) was predicted[16,17] and sequentially synthesized by arc discharge.[18] Theoretical and experimental studies have revealed many promising properties of BN-NTs for the development of BN-based nanotechnology.[19−25] In comparison with the carbon counterpart,[1−11] periodic BN nanostructures are still limited in the bamboolike BN-NTs, which were first observed in 1999 by annealing ball-milled hexagonal BN powders under NH_3.[26] A catalytic capillary growth mechanism was sequentially proposed.[27] Very recently, bamboolike BN-NTs were prepared via the carbothermal reduction of ultradispersed amorphous boron oxide in N_2 at 1100−1450 °C,[28] the heating of a mixture of boron and iron oxide in flowing ammonia gas,[29] the heating of a mixture of boron and alumina-supported nickel boride catalyst at 1400 °C under an NH_3 atmosphere,[30] and chemical vapor deposition using B-N-O precursors.[31,32]

By nitriding high-boron-content Fe-B nanoparticles with an ammonia/nitrogen (NH_3/N_2) gas mixture, we have reported the synthesis of BN nanowires.[33] In our case, which is different from the traditional vapor−liquid−solid (VLS) growth, in which catalyst particles act as the medium for transporting the component from vapor to solid,[9,34−36] the boron component in the BN nanostructure originates from the Fe-B "catalyst" itself, rather than from a vapor precursor. By replacing the high-boron-content Fe-B nanoparticles with the low-boron-content nanoparticles, in this paper, periodic spindle-unit BN-NTs have been obtained, in addition to regular cylindrical nanotubes. This novel BN nanostructure was well-characterized by high-resolution transmission electron microscopy (HRTEM) and energy-dispersive X-ray spectroscopy (EDX). Because of the simplicity of the preparation process, the formation of this type of periodic BN nanostructure could be reasonably deduced and an improved kinetic growth model of stress-induced sequential growth was proposed accordingly. The train of thought in this growth model could also be beneficial to understand the formation of some other periodic nanostructures.

Experimental Section

The preparation procedure is similar to that described in our previous work.[33] The only difference is that the Fe-B "catalyst" particles used here were prepared via a solution chemical reaction method with a low boron content of ∼30 at. %.[37] Briefly speaking, the Fe-B nanoparticles were placed evenly in an alumina crucible and positioned at the center of an alumina tube. A commercially available NH_3/N_2 gas mixture (4 mol % NH_3) with a flow rate of 100 sccm was introduced. After the reaction of the NH_3/N_2 gas mixture with the Fe-B nanoparticles

* Author to whom correspondence should be addressed. E-mail: zhenghu@nju.edu.cn.

10.1021/jp035375w CCC: $25.00
Published on Web 09/24/2003

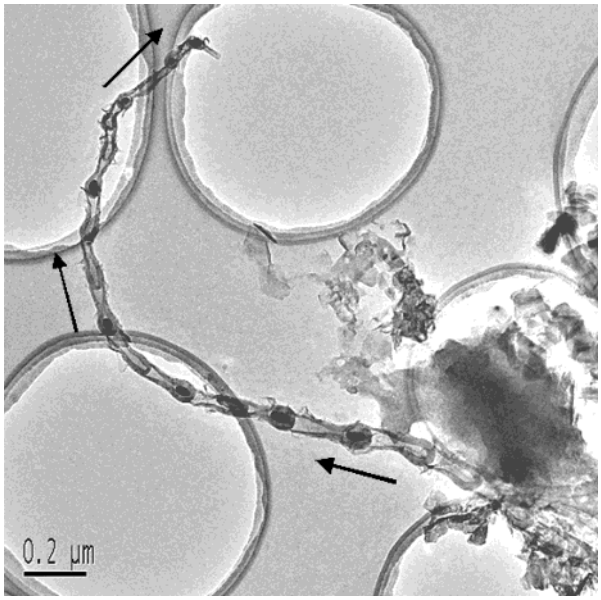

Figure 1. Typical TEM micrograph of the periodic spindle-unit BN nanotubes. Arrows indicate the growth direction.

at 1100 °C for 2 h, the alumina tube reactor was cooled to room temperature in an argon atmosphere. The obtained product resembled a slag that had adhered to the alumina crucible substrate, implying its molted state during reaction. The collected slag sample was well-characterized by HRTEM (JEOL, model JEM-2010). The chemical composition of the individual nanostructures was analyzed by EDX (ThermoNORAN) that was attached to the HRTEM equipment.

Results and Discussion

Figure 1 is a typical micrograph of the novel periodic BN nanostructures, which is made via repetition of the spindle-like unit. Most of the spindles are hollow-cored, and a few spindles contain nanoparticles inside the hemispherical-like ends. Figure 1 shows that the distribution of the inside nanoparticles is random. For each spindle unit, along the growth direction (as indicated by the arrow in Figure 1), the outer diameter decreases steeply and then increases gradually, accompanied by thinning of the wall thickness. In overview, the diameter of the spindle-unit nanotube shows a decreasing tendency along the growth direction. This is obviously different from the commonly observed bamboolike nanotubes with approximately constant outer diameter.[3−8,28−30] These features could be demonstrated more clearly in the HRTEM images in the following section.

Figure 2a is a typical HRTEM image of the spindle-like compartment. For such a typical unit, it is clearly shown that the wall thickness (indicated by arrow ①) decreases gradually and the BN layers at the inner and outer surface gradually disappear along the growth direction. The thinner end of the spindle-like compartment wall connects with the inner knot layers (indicated by arrow ②), resulting in the sudden increase of the wall thickness at the joint knot portion. Figure 2b is an enlarged view of the joint part in Figure 2a, revealing the joint structure in detail. The image shows that the spindle-unit BN-NT is well-crystallized with the lattice spacing between two neighboring fringes of ~0.34 nm, corresponding to the d_{0002} spacing in bulk hexagonal BN (0.333 nm).[15,33] Some defective BN sheets at the outer surface of the wall could be observed clearly in Figure 2b. The corresponding EDX spectrum (Figure 2c) of the compartment exhibits well-resolved signals from the characteristic K-shell ionization edges of boron at 188 eV and

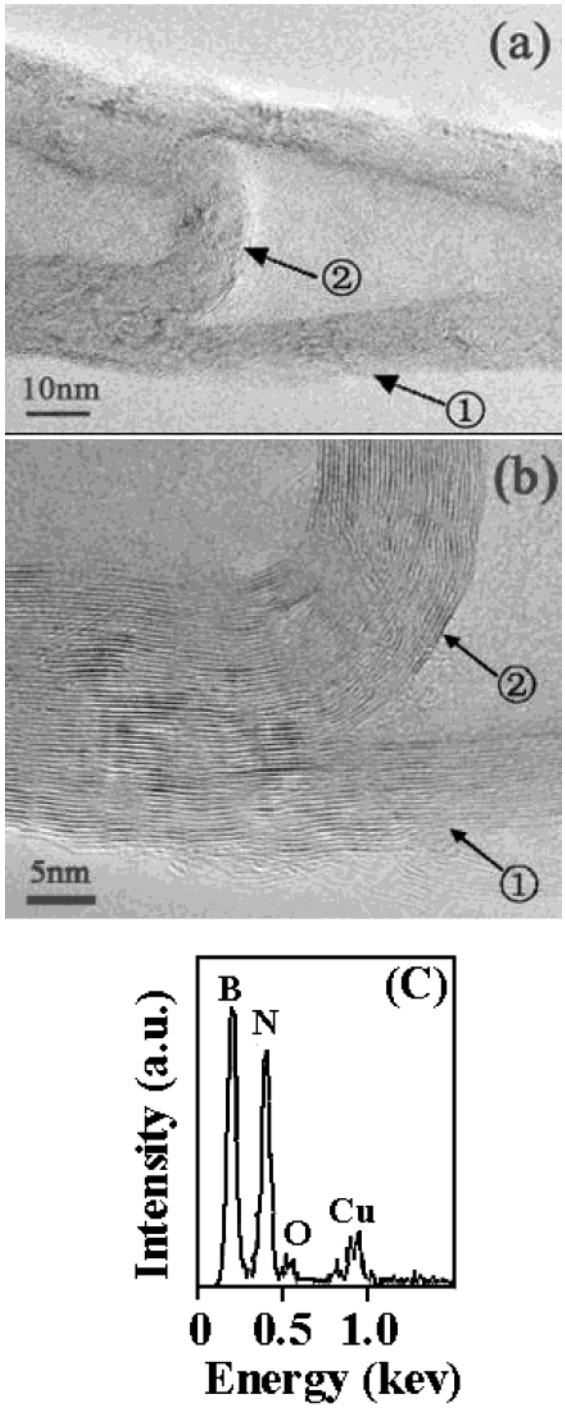

Figure 2. (a) HRTEM image of the typical spindlelike compartment. The wall (indicated by arrow ①) connects with the inner knot layers (indicated by arrow ②), resulting in the sudden increase of the wall thickness; (b) high-magnification image of the joint part in Figure 2a; (c) the corresponding EDX spectrum.

nitrogen at 400 eV, confirming that the compartment is pure BN. The weak signal at 530 eV is due to the oxygen adsorption during sample transfer through air, and the HRTEM copper sample grid causes the signal at 930 eV.

Figure 3a shows a high-magnification image of the spindle-like compartment that contains a nanoparticle inside the hemispherical-like end. The corresponding atom-resolved HR-TEM image and EDX analysis of the nanoparticle surrounded by the crystalline BN layers are shown in Figure 3b and c, respectively. The results clearly indicate that the encapsulated nanoparticle is an iron-containing "catalyst" that is surrounded

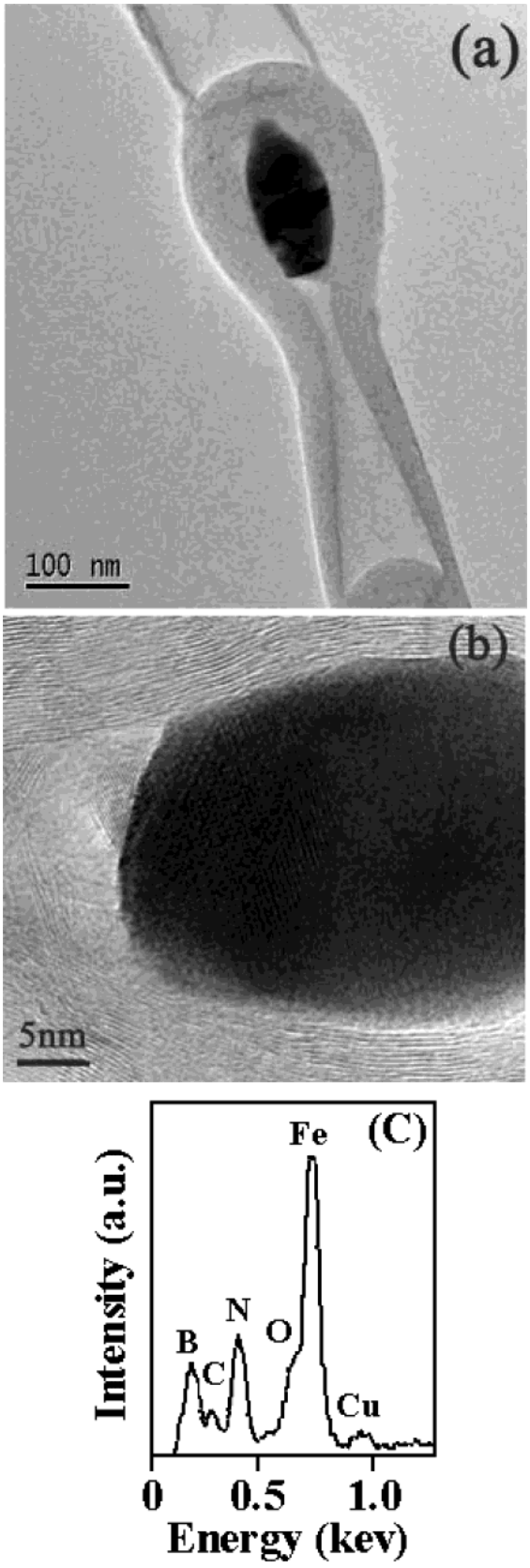

Figure 3. (a) Typical image of the spindlelike compartment with an iron-containing "catalyst" inside the hemispherical-like end. Panels b and c respectively show the corresponding atom-resolved HRTEM image and EDX spectrum of the "catalyst" surrounded by BN shells.

by well-crystallized BN layers. The shape of the encapsulated nanoparticle is reminiscent of a drop of mercury inside a glass capillary, which suggests that the nanoparticle should be in a liquid or quasi-liquid state during the reaction at 1100 °C. The contact angle between the nanoparticle and the inner wall of BN is >90°, which indicates poor compatibility between the nanoparticle and the BN substance. The signal peaks of B and N in Figure 3c should mainly originate from the outer BN layers. The weak signal at 530 eV is due to the oxygen adsorption during sample transfer through air, and the HRTEM copper sample grid and carbon film respectively cause the Cu and C signals. The encapsulation of catalyst particles inside the compartments is also observed for bamboolike CNTs in the literature.[11,27]

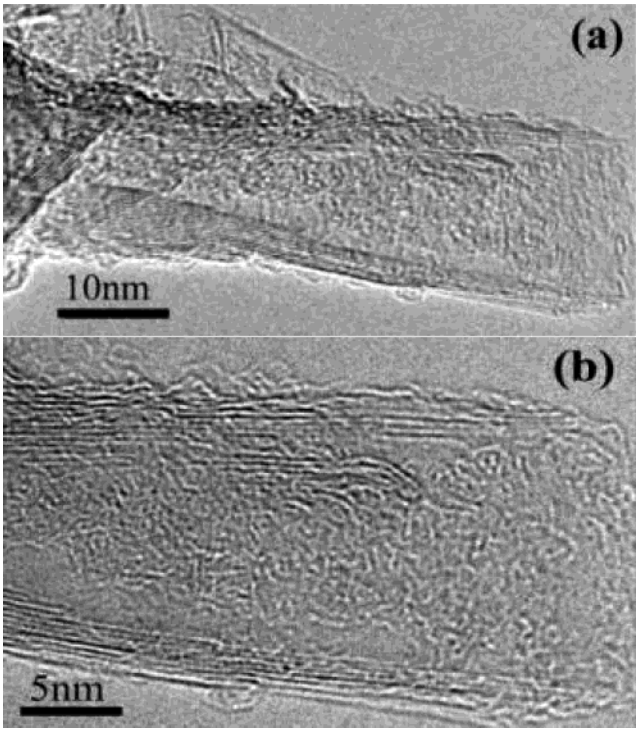

Figure 4. (a) HRTEM image of the tip portion of the spindle-unit nanotube in Figure 1; (b) enlarged HRTEM image of the buglelike tip structure.

The HRTEM image of the tip region, i.e., the last unit of the nanotube in Figure 1 is shown in Figure 4a. Figure 4b is an enlarged HRTEM image of the buglelike tip structure. In addition to all the common features for the spindle unit previously described, a special feature is that it has an open end that resembles a bugle. This structure was formed because the iron-containing "catalyst" nanoparticle desquamated from the BN tubular end, because of the increased interfacial energy between the nanoparticle and the BN layer. The increase in the interfacial energy resulted from the depletion of the boron content within the Fe-B "catalyst" particle[8] and the decreasing size of the "catalyst" particle,[38] accompanied by the growth of this nanotube.

The growth of these novel, periodic spindle-unit BN-NTs could be analogous to the VLS mechanism.[9,34−36] For the VLS mechanism, the liquid catalyst accepts the components from a vapor, causing the liquid catalyst to become supersaturated, and then the accepted components precipitate in whisker form. The difference in our case is that the Fe-B "catalyst" not only acts as the medium for transportation of the components from the vapor to the product (i.e., nitrogen from NH_3/N_2), as is the case in VLS growth, but also partially provides the component itself (i.e., boron from the Fe-B catalyst). Strictly speaking, Fe-B is not the "catalyst": rather, it is a reactant, because the boron component in Fe-B is consumed after the chemical reaction. In

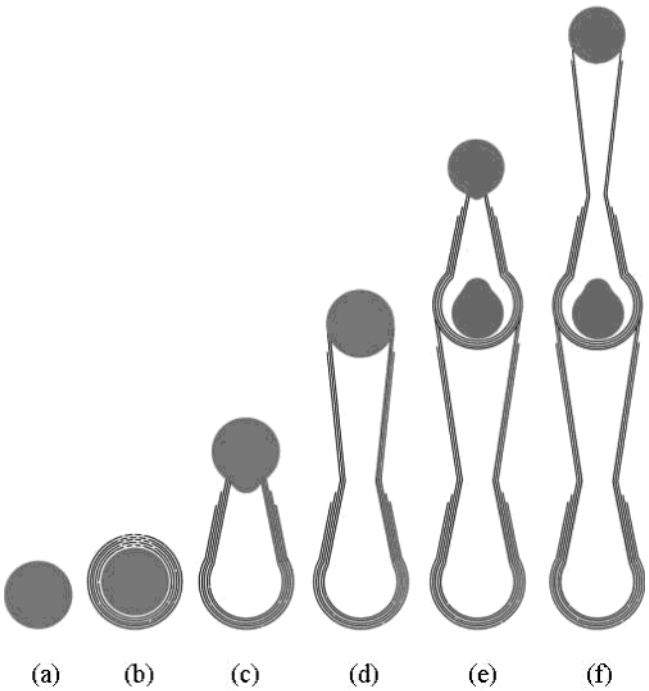

Figure 5. Schematic diagram of the improved stress-induced sequential growth model. (See text for details.)

our experiments, the nanosized Fe-B particle is confined by BN shells and an interface between the Fe-B "catalyst" and BN shells is formed, which could contribute to the total free energy of the nanoscale systems, resulting in the depression of the melting point of the Fe-B "catalyst".[12,39,40] The nanoscale size of the "catalyst" is also a favorable factor for decreasing its melting point.[35,41] Hence, although the reaction temperature of 1100 °C in our preparation is lower than the melting point of Fe-B alloy in bulk, the Fe-B "catalyst" should be in a molten or quasi-liquid state, as inferred from the morphology of the encapsulated iron-containing nanoparticles in Figure 3.

On the basis of the aforementioned experimental results and analysis, an improved stress-induced sequential growth mode for the formation of the periodic spindle-unit BN-NTs is proposed and illuminated schematically in Figure 5. At high temperature (~1100 °C), the Fe-B "catalyst" decomposes NH_3/N_2 on the surface to produce the N atoms, which diffuse into the Fe-B "catalyst" and combine with the B atoms to form the BN species (Figure 5a). When the BN species is supersaturated, it begins to precipitate layer by layer in the form of BN shells around the molten iron-containing (Fe-B-N) "catalyst" (Figure 5b), similar to the case presented in Fray's report.[42] With the inward growth of the BN layer between the interface of the formerly formed BN shell and the Fe-B-N core, the increasing curvature of the newly formed BN shell results in increasing stress energy between the BN shells and the Fe-B-N nanoparticle core.[8] When the stress energy reaches a certain degree, the molten Fe-B-N "catalyst" core will be expulsed from the defective region of the BN shell and sequentially shrink to locate on the door of the torn elongated BN shell, as shown in Figure 5c. The first part of the hollow-cored spindle with steeply decreasing outer diameter is then formed. The expelled Fe-B-N "catalyst" continues to precipitate the supersaturated BN species epitaxially at the joint region, and the tubular structure is formed sequentially (Figure 5d). Because of the gradually decreasing population of the supersaturated BN species inside the Fe-B-N "catalyst", the chemical potential of the dissolved BN decreases accordingly, which favors the tube growth with a low formation energy, i.e., with a large diameter.[11,16,17] Consequently, the wall thickness becomes thinner and the diameter becomes bigger progressively for the formed BN tubular structure, as shown in Figures 1, 2a, and 3a, as well as schematically shown in Figure 5d. This growth process stops when the concentration of the BN species inside the molten Fe-B-N "catalyst" is consumed, and the second part of the hollow-cored spindle is formed accordingly. The above-mentioned steps (i.e., Figure 5a−d) then are restarted with the same "catalyst" initially located at the end of the preceding circle. This process repeats again and again until the boron component within the "catalyst" is depleted or the "catalyst" desquamates from the BN layers. A series of spindles are then sequentially formed, which are connected one by one to form the periodic spindle-unit BN nanostructures. Note that, for the step depicted in Figure 5c, a splitting of the liquid "catalyst" could occur. Hence, the "catalyst" partially remains in the hemispherical-like end of certain spindles and the rest of the "catalyst" is expelled for the further growth of the BN-NT, as observed in Figures 1 and 3, as well as schematically demonstrated in Figure 5e and f. Roughly speaking, if we neglect the deformation of the hemispherical-like end of the spindles before and after the expulsion of the "catalyst", the inner dimension of a certain spindle should be determined by the "catalyst" volume when putting the "catalysts" after that spindle along the growth direction together. The molten "catalyst" is occasionally partially trapped inside some spindles, as revealed by Figure 1; therefore, the size of the "catalyst" capable of further growth of BN spindles becomes smaller and smaller. As a result, the diameter of the periodic spindle-unit nanotube shows a decreasing tendency along the growth direction, as clearly shown in Figure 1.

Because of the simplicity of our preparation procedure and the forthright HRTEM characterization, in the preceding discussion, an improved stress-induced sequential growth model has been reasonably deduced, with which the formation process of the novel spindle-unit BN nanostructure could be well understood. In comparison with relative stress-induced growth model, i.e., the compartment of the bamboolike nanotube is formed by the expulsion of catalyst or the detachment of tubular structure from the catalyst,[7−9,27] our model considers that the expulsion of the molten "catalyst" from BN shells due to stress only results in the formation of the first hemispherical-like portion of the spindle unit. The second portion of the spindle unit is formed by the following epitaxial growth of BN, because the BN species is still supersaturated inside the "catalyst" when the "catalyst" is just expelled.

Conclusion

In summary, novel, periodic spindle-unit BN nanotubes with buglelike open-end tips have been found in the product, simply by nitriding low-boron-content Fe-B nanoparticles with a N_2/NH_3 gas mixture at 1100 °C. The diameter of such a BN nanotube shows a decreasing tendency along the growth direction. For each spindle unit, the outer diameter decreases steeply and then increases gradually, accompanied by thinning of the wall thickness along the growth direction. These features are obviously different from the commonly observed bamboolike nanotubes with approximately constant outer diameter. Because of the simplicity of the preparation procedure and the forthright HRTEM characterization, an improved stress-induced sequential growth model has been reasonably deduced, with which the formation process of this novel nanostructure could be well understood. The train of thought in this growth model could also be beneficial to understand the formation of some other periodic nanostructures.

Acknowledgment. The financial support from the Natural Science Foundation of China (10175034), the Chinese Ministry of Education (No. 02110), and the National Key Project for High-Tech (No. 2003AA302150) are greatly acknowledged.

References and Notes

(1) Sun, Y. P.; Riggs, J. E. *Int. Rev. Phys. Chem.* **1999**, *18*, 43.
(2) Baughman, R. H.; Zakhidov, A. A.; De Heer, W. A. *Science* **2002**, *297*, 787.
(3) Seraphin, S.; Wang, S.; Zhou, D.; Jiao, J. *Chem. Phys. Lett.* **1994**, *228*, 506.
(4) Saito, Y. *Carbon* **1995**, *33*, 979.
(5) Lee, C. J.; Park, J. *J. Phys. Chem. B* **2001**, *105*, 2365.
(6) Li, Y. D.; Chen, J. L.; Ma, Y. M.; Zhao, J. B.; Qin, Y. N.; Chang, L. *Chem. Commun.* **1999**, 1141.
(7) Wang, X. B.; Hu, W. P.; Liu, Y. Q.; Long, C. F.; Xu, Y.; Zhou, S. Q.; Zhu, D. B.; Dai, L. M. *Carbon* **2001**, *39*, 1533.
(8) Zhang, X. X.; Li, Z. Q.; Wen, G. H.; Fung, K. K.; Chen, J. L.; Li, Y. D. *Chem. Phys. Lett.* **2001**, *333*, 509.
(9) Kukovitsky, E. F.; L'vov, S. G.; Sainov, N. A. *Chem. Phys. Lett.* **2000**, *317*, 65.
(10) Kovalevski, V. V.; Safronov, A. N. *Carbon* **1998**, *36*, 963.
(11) Jourdain, V.; Kanzow, H.; Castignolles, M.; Loiseau, A.; Bernier, P. *Chem. Phys. Lett.* **2002**, *364*, 27.
(12) Chen, Y.; Chadderton, L. T.; FitzGerald, J.; Williams, J. S. *Appl. Phys. Lett.* **1999**, *74*, 2960.
(13) Ma, R. Z.; Bando, Y.; Sato, T.; Golberg, D.; Zhu, H. W.; Xu, C. L.; Wu, D. H. *Appl. Phys. Lett.* **2002**, *81*, 5225.
(14) Ma, R. Z.; Bando, Y.; Sato, T. *Adv. Mater.* **2002**, *14*, 366.
(15) Paine, R. T.; Narula, C. K. *Chem. Rev.* **1990**, *90*, 73.
(16) Blasé, X.; Rubio, A.; Louie, S. G.; Cohen, M. L. *Europhys. Lett.* **1994**, *28*, 335.
(17) Rubio, A.; Corkill, J. L.; Cohen, M. L. *Phys. Rev. B* **1994**, *49*, 5081.
(18) Chopra, N. G.; Luyken, R. J.; Cherrey, K.; Crespi, V. H.; Cohen, M. L.; Louie, S. G.; Zettl, A. *Science* **1995**, *269*, 966.
(19) Azevedo, S.; Mazzoni, M. S. C.; Chacham, H.; Nunes, R. W. *Appl. Phys. Lett.* **2003**, *82*, 2323.
(20) Tang, C. C.; Bando, Y.; Ding, X. X.; Qi, S. R.; Golberg, D. *J. Am. Chem. Soc.* **2002**, *124*, 14550.
(21) Chopra, N. G.; Zettl, A. *Solid State Commun.* **1998**, *105*, 297.
(22) Chen, R. B.; Shyu, F. L.; Chang, C. P.; Lin, M. F. *J. Phys. Soc. Jpn.* **2002**, *71*, 2286.
(23) Pokropivnyi, V. V. *Powder Metall. Met. Ceram.* **2001**, *40*, 582.
(24) Ma, R. Z.; Bando, Y.; Zhu, H. W.; Sato, T.; Xu, C. L.; Wu, D. H. *J. Am. Chem. Soc.* **2002**, *124*, 7672.
(25) Meunier, V.; Roland, C.; Bernholc, J.; Nardelli, M. B. *Appl. Phys. Lett.* **2002**, *81*, 46.
(26) Chen, Y.; Gerald, J. F.; Williams, J. S.; Bulcock, S. *Chem. Phys. Lett.* **1999**, *299*, 260−264.
(27) Chadderton, L. T.; Chen, Y. *J. Cryst. Growth* **2002**, *240*, 164.
(28) Pokropivny, V. V.; Skorokhod, V. V.; Oleinik, G. S.; Kurdyumov, A. V.; Bartnitskaya, T. S.; Pokropivny, A. V.; Sisonyuk, A. G.; Sheichenko, D. M. *J. Solid State Chem.* **2000**, *154*, 214.
(29) Tang, C. C.; de la Chapelle, M. L.; Li, P.; Liu, Y. M.; Dang, H. Y.; Fan, S. S. *Chem. Phys. Lett.* **2001**, *342*, 492.
(30) Tang, C. C.; Bando, Y.; Sato, T. *Chem. Phys. Lett.* **2002**, *362*, 185.
(31) Ma, R. Z.; Bando, Y.; Sato, T.; Bourgeois, L. *Diamond Relat. Mater.* **2002**, *11*, 1397.
(32) Ma, R. Z.; Bando, Y.; Sato, T. *Adv. Mater.* **2002**, *14*, 366.
(33) Huo, K. F.; Hu, Z.; Chen, F.; Fu, J. J.; Chen, Y.; Liu, B. H.; Ding, J.; Dong, Z. L.; White, T. *Appl. Phys. Lett.* **2002**, *80*, 3611.
(34) Wagner, R. S.; Ellis, W. C. *Appl. Phys. Lett.* **1964**, *4*, 89.
(35) Morales, A. M.; Lieber, C. M. *Science* **1998**, *279*, 208.
(36) Pan, Z. W.; Dai, Z. R.; Ma, C.; Wang, Z. L. *J. Am. Chem. Soc.* **2002**, *124*, 1817.
(37) Hu, Z.; Han, Y.; Chen, F.; Chen, Y. *J. Chem. Soc.: Chem. Commun.* **1995**, 247.
(38) Adamson, A. W.; Gast, A. P. *Physical Chemistry of Surface*, 6th ed.; Wiley: New York, 1997.
(39) Navascues, G.; Tarazona, P. *Mol. Phys.* **1987**, *62*, 497.
(40) Jiang, Q.; Aya, N.; Shi, F. G. *Appl. Phys. A* **1997**, *64*, 627.
(41) Goldstein, A. N.; Echer, C. M.; Alivisatos, A. P. *Science* **1992**, *256*, 1425.
(42) Warner, T. E.; Fray, D. J. *J. Mater. Sci.* **2000**, *35*, 5341.